IEEE Access
Multidisciplinary | Rapid Review | Open Access Journal

Received May 22, 2020, accepted June 4, 2020, date of publication June 11, 2020, date of current version June 23, 2020.

Digital Object Identifier 10.1109/ACCESS.2020.3001903

Design of a Rectenna Array Without a Matching Network

THAMER S. ALMONEEF, (Member, IEEE)
Electrical Engineering Department, College of Engineering, Prince Sattam Bin Abdulaziz University, Al-Kharj 11942, Saudi Arabia
e-mail: t.almoneef@psau.edu.sa

This work was supported by the Deanship of Scientific Research at the Prince Sattam Bin Abdulaziz University under the Research Project 2019/01/10795.

ABSTRACT A novel approach to designing rectenna systems by eliminating the use of a matching network between the antenna and the rectifier is presented. The proposed rectenna consists of a wide impedance bandwidth 8 octagon disks placed at two different layers laying on both sides of a single substrate and backed by a ground plane. A Schottky diode is placed at each layer right at the feeding location without matching network, forming an array of two rectennas. The rectified power is smoothed out using a low pass filter composed of two RF choke inductors for each rectenna. By virtue of the wide impedance bandwidth of the antenna, the measurement results of the rectenna yielded a 50% radiation to DC efficiency at the operating frequency of 2.1 *GHz*. The rectifiers were then connected in series or parallel to study the effect of the connection type on the rectified output power. Wideband load resistance response and configurable amount of output DC currents and voltages can be realized using certain DC power combining methods.

INDEX TERMS Rectenna, rectifying antenna, energy harvesting, microwave rectifiers.

I. INTRODUCTION

A rectifying antenna (rectenna) consists mainly of an antenna to convert electromagnetic energy to AC power and a rectifier that converts the collected AC power to DC. Such rectenna system is an integral and critical part of Wireless Power Transfer systems (WPT). Since their main goal is to deliver energy wirelessly to a load, rectennas enabled numerous applications such as Space Solar Power [1], [2], energy harvesting/scavenging [3]–[5], remote sensing [6], [7], Internet Of Things (IOT) [8]–[10], wireless battery charging [11], and infrared detection [12], [13].

The conventional rectenna system consists of 5 main parts as shown in Fig.1(a). The antenna first captures the electromagnetic energy and then converts it to AC power. A bandpass filter is then used to match the antenna impedance to that of the diode. The diode then converts the AC power collected by the antenna to DC. A low pass filter is used beyond the diode to filter high order harmonics and smooth out the rectified power before it is delivered to the load. The radiation to DC conversion efficiency is considered the most important figure of merit to evaluate the performance of any rectenna system. The total efficiency is effected by the individual efficiencies of each part of the rectenna namely: an antenna, a matching network between the rectifier and the antenna, a diode and a low pass filter. In addition, the total efficiency is greatly effected by the input power level, the operating frequency and the optimal terminated load resistance.

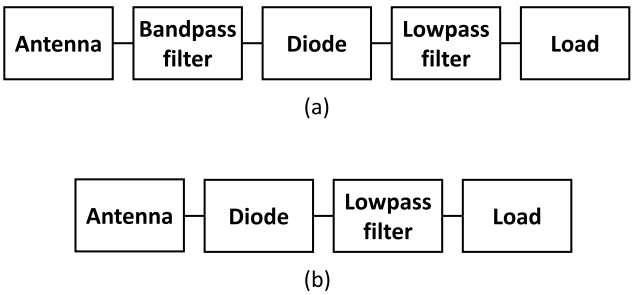

FIGURE 1. Block diagram of (a) the conventional rectenna, and (b) the proposed rectenna.

In the literature, the work in [14], [15], focused on analysing and enhancing the efficiency of the antenna by using metasurfaces with radiation to AC efficiencies approaching unity. Others concentrated on designing rectifiers with AC to DC efficiencies exceeding 70% [16], [17]. The work presented in [18], [19] developed full rectenna

The associate editor coordinating the review of this manuscript and approving it for publication was Aijun Yang.

systems with radiation to DC efficiencies of more than 80%. Depending on the desired application, a rectenna can be designed to have wide frequency response [20]–[22], wide load impedance response [23], multiband operation [24], high output voltage [25], dual polarized [26] or low input power operation [27].

The use of a matching network between the antenna and the diode is critical to maximally transfer the energy from the antenna to the diode. Such matching network can add to the losses of the total efficiency of the system in addition to narrowing the overall operating frequency band. The overall size is also increased since most matching networks have to be approximately $\lambda/2$ in size [28], [29]. It is sometimes desired to eliminate the matching network between the antenna and the diode to avoid the narrow band effect, the losses of the matching network and miniaturise and simplify the overall rectenna design. The work in [30] presented a broadband rectenna made of spiral antennas and the diodes were mounted right at the feed of each antenna without a matching network to avoid the narrow band effect of the matching circuit. However, the efficiency was limited to 20% for input power levels of 0.07 mW/cm^2 due to the high impedance mismatch between the diode and the antenna. Another technique was used in [31], [32] where the antenna is designed such that its input impedance is conjugate matched to the diode impedance, thus the diode can be placed at the feed of the antenna without utilizing a matching network.

In this work, a novel and simple approach to designing rectenna systems without a matching network is presented. Note that the conjugate matching technique used previously is based on analysing the input impedance of the diode, which usually has the form of a resistance and a capacitive behaviour such that $Z(diode) = R - jX$, then an antenna is designed to have an input impedance that is conjugate matched to that of the diode impedance such that $Z(antenna) = R + jX$. This provides matching over a single frequency and a matching network can be eliminated. In addition, this technique works for the particular diode that is used to conjugate match the antenna. If another diode is desired, the antenna design must be modified to accommodate the impedance of the new diode. In the proposed design technique, the antenna input impedance is not conjugate matched to that of the diode, but rather it is designed to have a wideband impedance response such that when a diode is mounted across its feed, significant energy transfer occurs between the antenna and the diode. In addition, the diode can be mounted without analyzing its impedance since most diodes have a real part input impedance in the range of the input impedance of the antenna. Once rectified, the power is smoothed out using carefully selected inductor with low series resistance and high self-resonance frequency relative to the operating frequency. Therefore, the proposed rectenna model is presented in the modified block diagram shown in Fig.1(b). The output DC power of the two rectennas presented in this paper were connected in both series and parallel and the advantages of both types of connections are discussed.

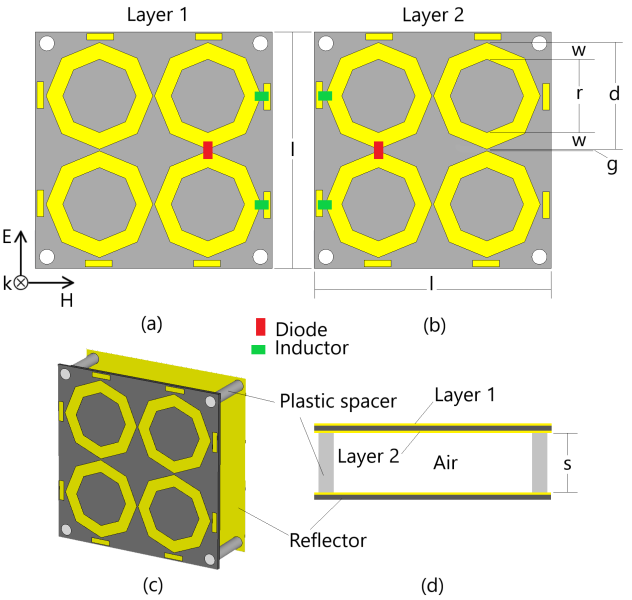

FIGURE 2. The proposed rectenna showing (a) top view of layer 1, (b) top view of layer 2, (c) perspective view, and (d) side view.

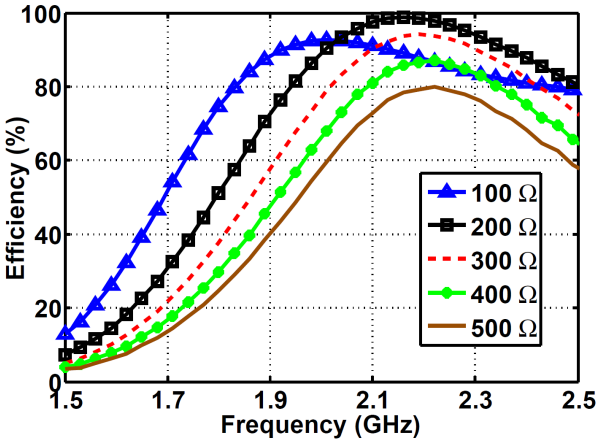

FIGURE 3. Numerical results showing the efficiency of the proposed antenna with various terminated loads ranging from 100 Ω to 500 Ω.

II. SIMULATION AND DESIGN

The proposed rectenna consists of two layers on an RT/duroid 5880 Rogers substrate material with a thickness of 1.6 *mm* as shown in Fig.2. Each layer contains four octagon loops with two loops used as parasitics while the other two loops are utilized for receiving electromagnetic energy from the gap g = 0.5 *mm* that is between the loops as labeled by "diode" in Fig.2(a) and (b). With reference to Fig.2, each octagon has dimensions of w = 5 *mm*, r = 22 *mm*, d = 32 *mm* and a side length of l = 71 *mm*. A reflector is placed at a distance s = 20 *mm* away from layer 2 and supported by four plastic spacers. The feed point of the second layer is placed below the parasitic elements of the first layer. This is critical to provide strong coupling between the two layers.

The proposed antenna was simulated in CST [33] in the receiving mode with a planewave excitation such that the

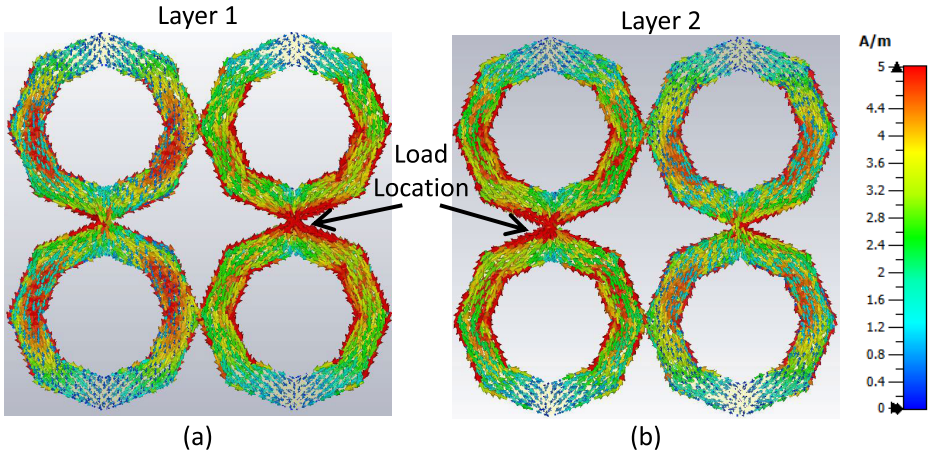

FIGURE 4. The current distribution on the surface of the proposed antenna for (a) first layer, and (b) second layer.

propagation direction is perpendicular to the plan of the layers as shown in Fig.2. Two variable resistive elements were placed at the feed point of each layer and the microwave to AC efficiency of the antenna is computed. Here, the value of each lumped element is the same in any simultaneous simulation run (e.g. if the lumped element of the first layer is assigned 200 Ω then the lumped element of the second layer will also be 200 Ω). Note that, the lumped element resistor will later be replaced by a diode to convert the collected AC power to DC and it is used here to analyse the response of the antenna efficiency to various load resistances. Figure 3 shows the efficiency of the antenna in the receiving mode with polarization as shown in Fig.2(a). The numerical results show that the antenna is capable of capturing electromagnetic waves with wide range of load resistances from 100 Ω to 500 Ω. At the resonance frequency of 2.2 *GHz*, the antenna is capable of collecting electromagnetic energy with efficiencies exceeding 80%. Here, the collected energy is the sum of the total energy received by the two layers. The fact that the proposed antenna can receive electromagnetic energy with high efficiencies at various terminated load impedances is a very critical feature for rectennas since a matching network can be avoided and a wide range of diode types can be placed across the feed of the antenna with sufficient power transfer between the antenna and the diode.

A simulation was then extended to understand how the antenna performs in the transmitting mode. The scattering parameters, showing the return loss of each layer and the insertion loss between the two layers, are presented in Fig.5. This simulation was performed with ports having impedance of 200 Ω which is the impedance that resulted in the highest received power. From the result, we can observe that close to the resonance frequency, almost half of the power is accepted by both layers. This shows that each layer is equally responsible for the total power received by the antenna as depicted in Fig.3. In addition, the curve of the insertion loss between the two layers show sufficient coupling between the two layers due to the close proximity of the two ports.

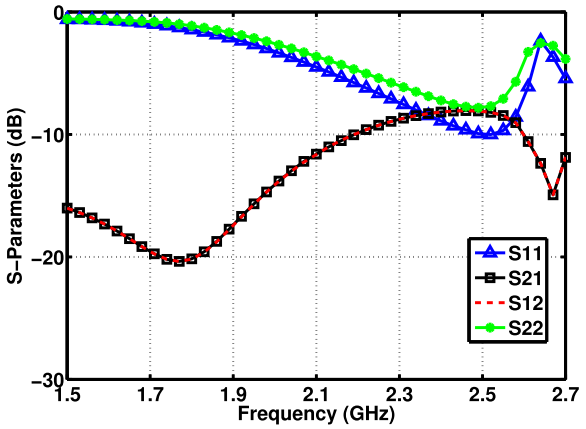

FIGURE 5. Simulation results of the proposed antenna in the transmitting mode showing the scattering parameters of the two layers.

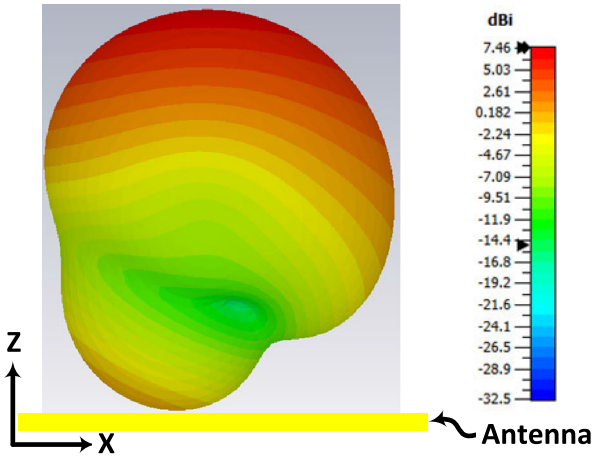

FIGURE 6. Simulation results of the proposed antenna in the transmitting mode showing the total gain of the antenna in dBi.

Figure 6 shows the gain of the antenna at the resonance frequency having a peak of 7.46 *dB*. Due to the presence of the ground plane, it is clear that most of the power is transmitted/received maximally from the broadside direction.

The current distributions along the surface of the octagons for the two layers are presented in Fig.4. The current was plotted in the range between 0 A/m to 5 A/m at the resonance frequency of 2.2 *GHz*. We can observe that high current is coupled to the loops at the resonance frequency. The current is much higher at the octagons that contain the load. In addition the current is highly concentrated across the load location of the two layers due to the high energy transfer from the octagons to the load of each layer. It is interesting to note that the other parasitic octagons also developed high surface current which aided in the wide impedance response of the antenna and the high conversion efficiency along a vast range of load impedances. This is due to the high coupling among the octagons located within the same layer and between the two layers. Note that the four octagons at each layer are tightly coupled having a separation distance of $\lambda_o/272$. Because they are tightly coupled, the current developed along the octagons is coupled to the main elements containing the load, and therefore most of the captured energy is consumed across the load. Utilizing highly coupled parasitic elements enables using less diodes per footprint which results in lower overall losses and lower input power requirements to turn on the diode since all the collected power per layer is channeled to one diode.

III. EXPERIMENTAL VALIDATION

To validate the proposed concept, the antenna designed above is fabricated and tested as in Fig.7. A pair of SMS7621-001LF Skyworks Schottky diodes were mounted at each layer right at the feed of the antenna without a matching network as shown in Fig.7. The output of the anode and the cathode sides of each diode were connected to a pair of 120 *nH* SMT L-14CR12JV4T inductors to pass the rectified DC power and prevent the AC power from reaching the load. The inductor was chosen carefully to ensure that its self resonance (23 *GHz*) is much greater than the operating frequency of (2.2 *GHz*) in addition to a low series DC resistance of 0.22 Ω to reduce the losses. Note that the inductor will have a minimal effect to the antenna performance since it is approximately an open circuit at the operating frequency of 2.2 *GHz*. The rectenna was placed a distance of 1 *m* away from a log periodic transmitting antenna array. A 3 *GHz* signal generator was connected to the transmitting antenna through a 36 *dB* gain high power amplifier.

In the experiment, the DC outputs of each diode from the two layers were connected first in parallel and then in series. For each connection type, a resistance sweep test was performed at the optimal power level and the optimal frequency as shown in Fig.8(a) and (b) for parallel and series connections, respectively. When the rectennas of layer 1 and layer 2 are connected in series, a wider impedance bandwidth can be observed as compared to the parallel connection case. This is due to the fact that when the two rectennas are connected in series, the optimal resistance of the two layers almost doubles. To understand this conclusion, let the optimal terminated load resistance of each rectenna to be R.

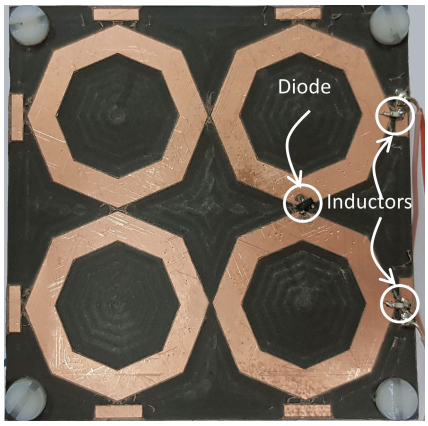

(a)

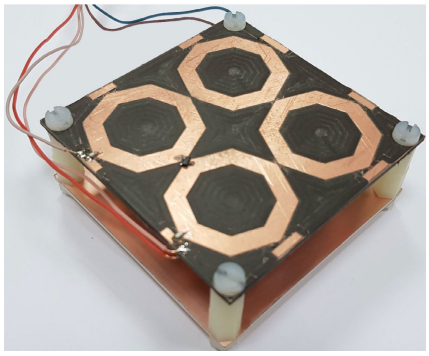

(b)

FIGURE 7. A photo showing the fabricated antenna (a) top view, and (b) perspective view.

Here, since the rectennas are of identical size, we can assume that both rectennas have an optimal resistance of R. When the two rectennas are connected in series, the total optimal load resistance is expected to double to a value of 2R. From Fig.8(b), the optimal resistance of the series connection type is 650 Ω, which gives a resistance of each layer rectenna to be R = 650/2 = 325 Ω. For parallel connection, the total optimal resistance can be expected to be R/2 = 162.5 Ω which is what the results have revealed in Fig.8(a). Thus, by connecting the two rectennas in series, the optimal resistance out of the two rectennas shifts up by a factor of 4 when compared to the parallel case causing the curve to have a wider impedance response with respect to the radiation to DC efficiency of the rectenna array.

Then, the input power was swept at the optimal load resistance and operating frequency. Figure 9 shows the input power variation as a function of efficiency. It is noticeable that both curves for the parallel and the series connection cases overlap having a peak efficiency of 50% at a power level of 29 dBm/m^2. This shows that, different from the resistance sweep, the connection type has no effect on the input power levels.

A frequency sweep was then performed as a function of efficiency at the optimal load resistance and power level for parallel and series connections as in Fig.10. The curves peak

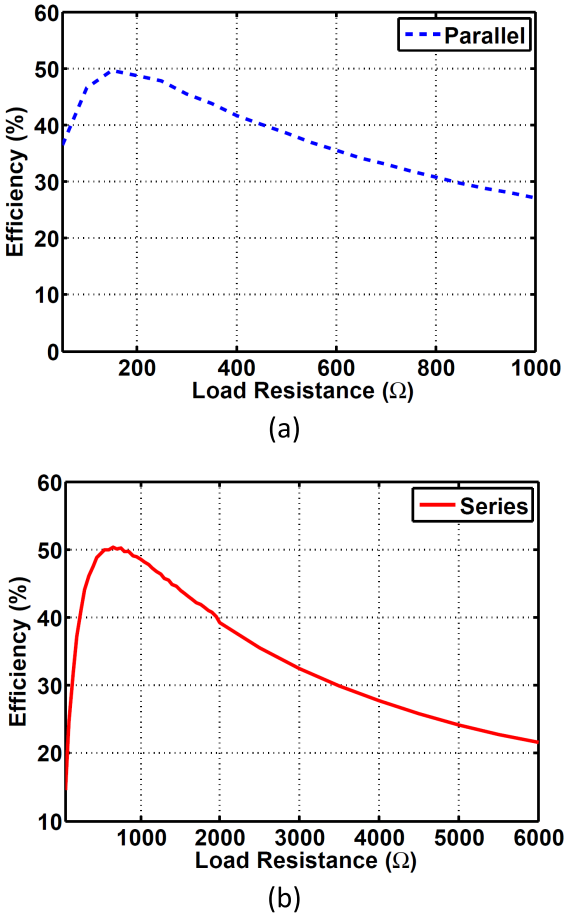

FIGURE 8. Experimental results showing the resistance sweep as a function of efficiency for (a) parallel and (b) series connections.

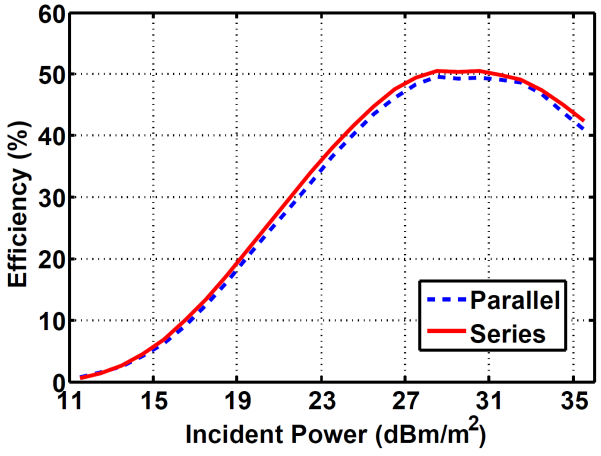

FIGURE 9. Experimental results showing the input power sweep as a function of efficiency for parallel and series connections.

at 2.1 *GHz* for both connection types with a slight shift of 100 *MHz* from simulated results due to fabrication tolerances. The efficiency of the measured rectenna at the resonance frequency has dropped to 50% as compared to a minimum efficiency of 80% for the simulated results. This can be attributed to the losses during the AC to DC power conversion of the

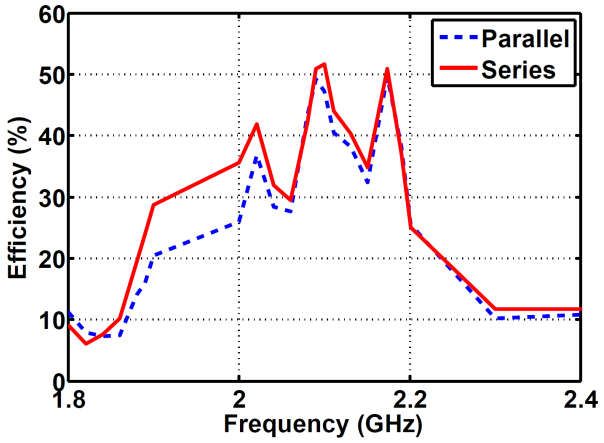

FIGURE 10. Experimental results showing the frequency sweep as a function of efficiency for parallel and series connections.

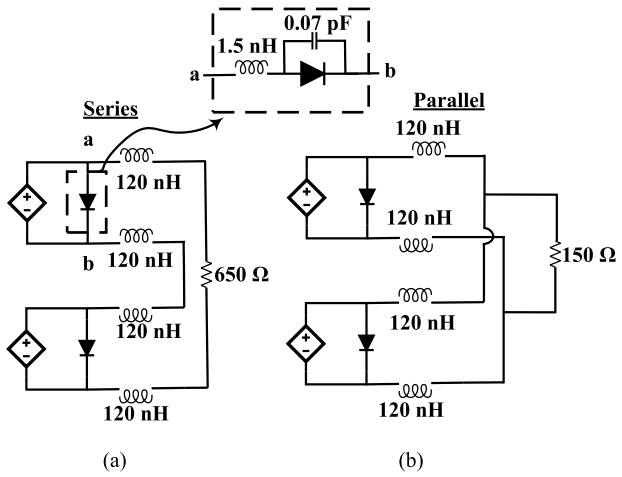

FIGURE 11. An equivalent circuit for the rectenna when the layers are connected in (a) series and (b) parallel.

diode, in addition to the losses at the harmonics frequencies which are generated due to the nonlinearity of the diode.

The equivalent circuits for both the series and parallel connected rectenna are shown in Fig.11. The voltage developed across the antenna feed of each layer is modeled as a dependent voltage source. This voltage is dependent on the frequency of operation, the power level available on the surface of the rectenna and the angle of incidence of the incoming wave. Note here that the operating frequency of 2.2 *GHz* is chosen as a proof of concept, however one can easily scale the antennas to operate at the desired frequency. The diode is connected in parallel to the antenna feed and the anode and cathode sides of each diode are connected to an inductor. Note here that the power after the inductor is purely DC since the chosen inductor acts as an open circuit at higher frequencies and short circuit at DC. After the inductors, the layers can be easily connected just like the output of two batteries combining the voltage if connected in series (Fig.11a) or boosting the current if connected in parallel (Fig.11b). The highlighted inset shows the Schottky diode equivalent circuit considering the parasitic effect of the packaging.

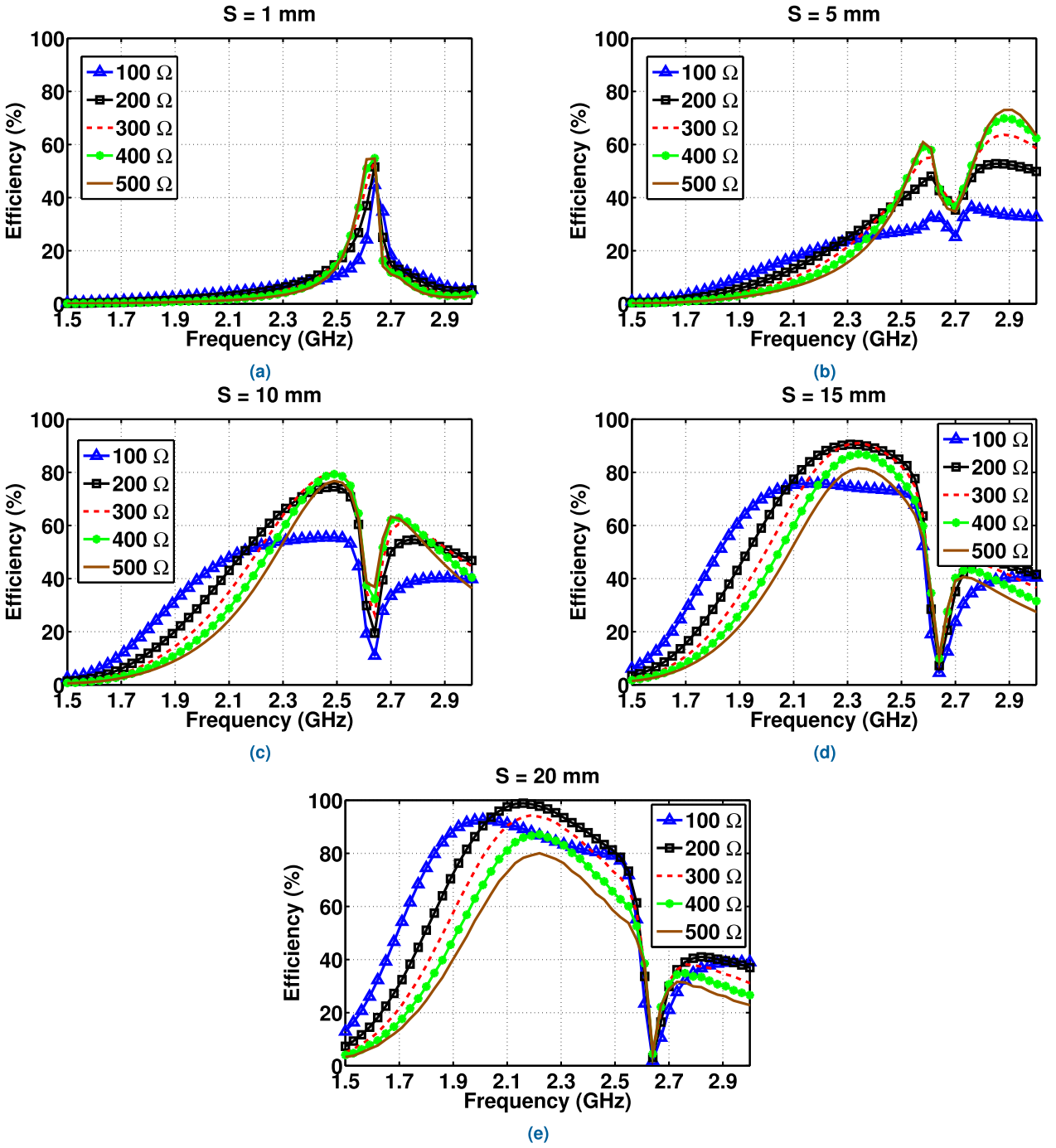

FIGURE 12. Numerical results showing the efficiency of the proposed antenna with various terminated loads ranging from 100 Ω to 500 Ω, and having a separation distance of (a) S = 1 mm, (b) S = 5 mm, (c) S = 10 mm, (d) S = 15 mm and (e) S = 20 mm.

From the measurement results, it is evident that regardless of the connection type, the input power, the operating frequency and the efficiency will always be the same. However, the connection type has a great impact on the optimal load resistance with an advantage of using series connection which results into a wideband load impedance response as compared to the parallel one. The best choice of connection type depends greatly on the type of load connected across the rectenna. To illustrate this further, Table1 shows the currents and voltages across the load resistances for both connection types. When the rectennas are connected in parallel, the current almost doubles compared to the series case. Conversely, the voltage across the load doubles when the rectennas are connected in series. Therefore, the type of connection can be chosen depending on the current and voltage requirements of the connected load.

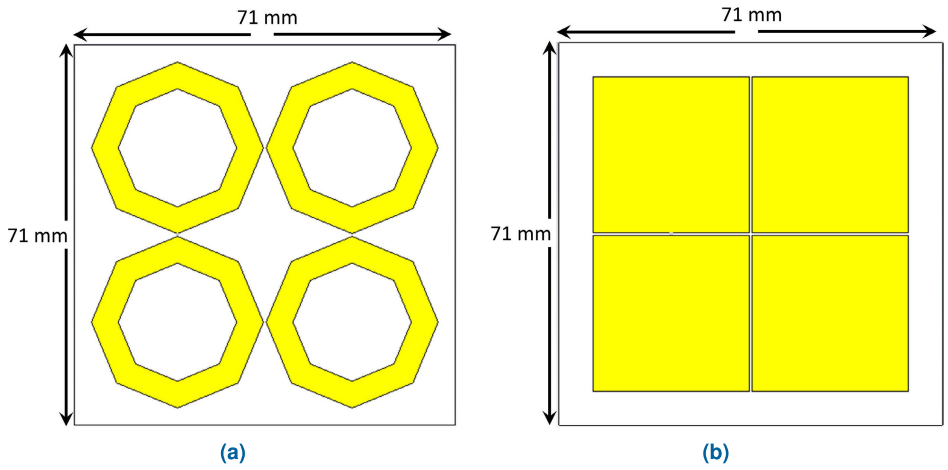

FIGURE 13. A schematic showing (a) the proposed 2 × 2 octagon array and (b) a 2 × 2 patch antenna array. Both arrays have a footprint area of 5,041 mm^2.

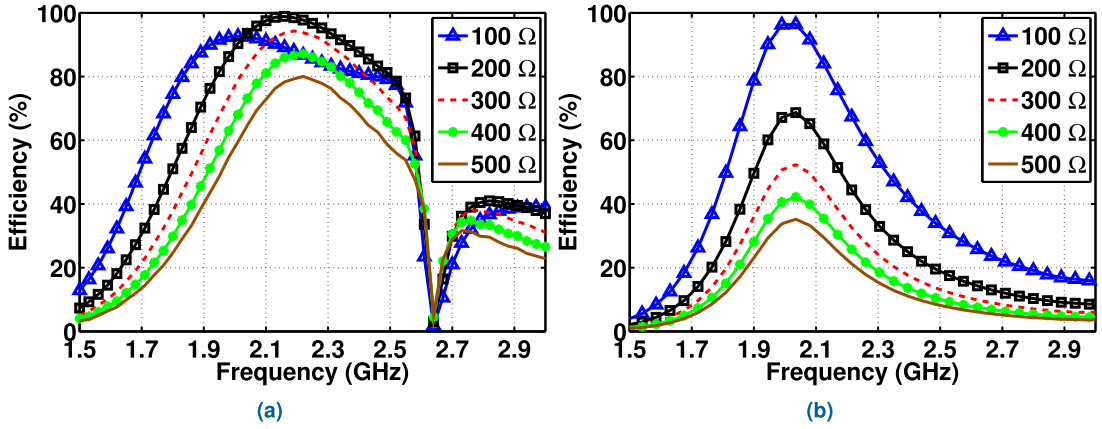

FIGURE 14. Numerical results showing the efficiency of the proposed antenna with various terminated loads ranging from 100 Ω to 500 Ω, and having a separation distance of S = 20 mm for (a) the proposed 2 × 2 octagon array and (b) a 2 × 2 patch antenna array.

TABLE 1. Voltage and current across the load for each connection type.

Connection	Current (mA)	Voltage (mV)	Load (Ω)
Parallel	3.22	516	150
Series	1.67	1087	650

IV. DISCUSSION

In Fig.3, the results showed that the antenna is capable of receiving at least 80% of the impinged energy on the surface of the antenna with wide range of impedances. To understand the main contributor to this wideband response, two numerical simulations were carried out. First, the distance between the reflector and the two-layer octagon antenna array was varied from $S = 1\ mm$ to $S = 20\ mm$ (please refer to Fig.2 for the definition of the separation distance (S)). In all separation cases, the load resistance was varied from 100 Ω to 500 Ω and the efficiency was recoded for a range of frequencies. Figures 12(a), 12(b), 12(c), 12(d), and 12(e) show the curves of the efficiency over frequency for a range of impedances with separation values of $S = 1\ mm$, $S = 5\ mm$, $S = 10\ mm$, $S = 15\ mm$ and $S = 20\ mm$, respectively. When the reflector is close to the antenna, the efficiency and the bandwidth degrades significantly. This is due to the fact that when the wave is reflected by the ground plane, the phase of the wave is reversed, causing both the ''imaged'' current on the reflector and the current on the antenna to cancel out. However, once the separation distance increases the performance of the antenna gradually improves in terms of impedance bandwidth, efficiency and frequency bandwidth. The optimal separation distance is when $S = 20\ mm$ which is approximately equivalent to a distance of $\lambda/4$. When the reflector is quarter wavelength apart from the antenna, the path of the incident wave from the antenna to the reflector and back to the antenna provides a full cycle, therefore both the original wave and the reflected wave are combined constructively, improving the overall performance of the antenna [35].

Another important factor that contributed to the efficiency and the impedance bandwidth of the proposed antenna is the shape of the cell. To illustrate this, a comparative study is conducted between the proposed antenna and a patch array of identical footprint size and the same number of cells

TABLE 2. A comparative study of various state of the art papers.

Ref.	Peak Freq. (GHz)	Antenna type	Eff. (%)	Matching network eliminated?	Matching network elimination technique	Diode type	Footprint (mm^2)	Single/ Array	Scalable output voltage and current
[30]	2-18	Spiral	20	Yes	50 ohm input impedance	SMS 7630	34,225	Array 8x8	No
[34]	2.45	Coplanar antenna	75	Yes	Conjugate matching	HSMS-2852	6,960	Single	No
[31]	2.75	Folded dipole	50	Yes	Conjugate matching	HSMS 2860	28,600	Array 4x4	Yes
[32]	0.98	Off-centered fed dipole	75	Yes	Conjugate matching	Variable	10,000	Single	No
[15]	2.7	Vivaldi	60	Yes	Conjugate matching	HSMS 2860	40,000	Array 4x4	No
This paper	**2.2**	**Octagonal**	**50**	**Yes**	**Wide impedance response**	**SMS 7621**	**5,041**	**Array 2x2**	**Yes**

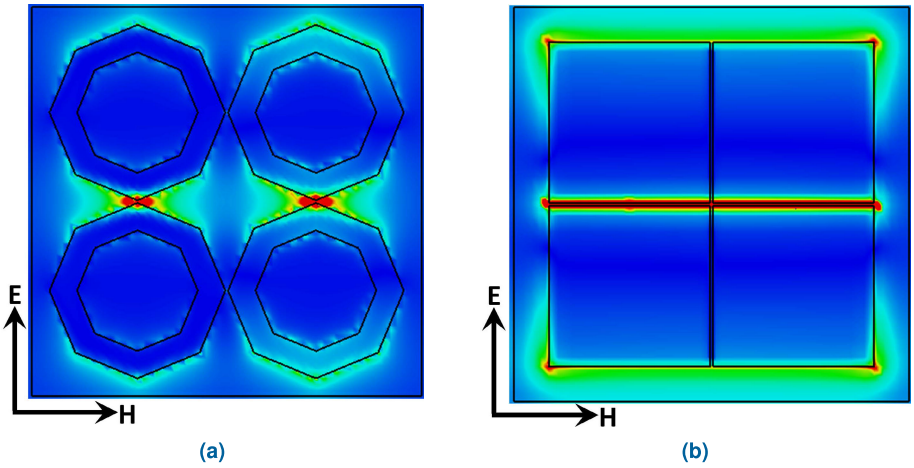

FIGURE 15. A contour plot of the electric field on the surface of (a) the proposed 2 × 2 octagon array and (b) a 2 × 2 patch antenna array. The field plot ranges between 0 V/m (blue) and 5 kV/m (red).

and layers as shown in Fig.13. To ensure fair comparison, both arrays were hosted on the same substrate and having identical separation distance of $S = 20\ mm$. The numerical results of both arrays are shown in Fig.14. The curves show that although the square patch and the octagon arrays were simulated in identical dimensions and electromagnetic environment, the efficiency of the square patch array drops as the impedance increases beyond 100 Ω. However, the array consisting of the octagon cells was able to maintain a minimum of 80% efficiency when the load impedance is increased up to 500 Ω. To shed some light on why this is happening, the electric field plots on the surface of both arrays is presented in Fig.15. From the field contour plot, we can see that the electric field is highly concentrated between the cells, which is the location of the feed for both arrays. However, for the patch array, the load experiences a uniform E-field along the separation between the two adjacent square patches. For the octagon on the other hand, the load sees a variable capacitive effect resulting on a variable E field due to the triangular edge like shape of the octagons. Such variable capacitance effect aided in widening the bandwidth of the impedance from the feed point of view.

The advantages of the rectenna presented in this paper is compared to that of rectennas in a number of published papers and summarized in Table 2, to further highlight the novelty of the proposed rectenna. Most of the listed papers utilize the technique of conjugate matching between the antenna and the diode. However, for this proposed paper, the octagon array antenna provides a wide impedance bandwidth allowing flexibility of using a wide range of diodes without a matching network and without considering the input impedance of the diode. Although the proposed antenna is made of an array of 2 × 2, its footprint size is relatively small. This can be attributed to the antenna design having the cells being tightly coupled, in addition to eliminating the matching network and the use of a simple lumped element inductor as an output low pass filter. One critical advantage is the configurability of the total output current and voltage which can be varied according to the load requirements. This adds a critical feature having a flexible rectenna that can fulfil the desired output requirements of a certain load.

V. CONCLUSION

A rectenna design with wideband input impedance response was presented. Such design allows for eliminating the use of a matching network between the antenna and the diode, thus a wide range of diodes can be used and mounted right the feed of the antenna. The rectenna design was validated experimentally having efficiencies of 50% at the operating frequency of 2.1 *GHz* for both connection types. Furthermore,

the two diode outputs were connected in series and parallel to study the advantages of both connections. Such design can be scaled to a larger array with a combination of connection types to achieve the total current and voltage that drives the desired load.

REFERENCES

[1] P. E. Glaser, "Power from the sun: Its future," *Science*, vol. 162, no. 3856, pp. 857–861, Nov. 1968.

[2] R. Erb, "Power from space—The tough questions: The 1995 Peter E. Glaser lecture," *Acta Astronautica*, vol. 38, nos. 4–8, pp. 539–550, 1996.

[3] S. D. Assimonis, V. Fusco, A. Georgiadis, and T. Samaras, "Efficient and sensitive electrically small rectenna for ultra-low power RF energy harvesting," *Sci. Rep.*, vol. 8, no. 1, pp. 1–13, Dec. 2018.

[4] B. Strassner and K. Chang, "5.8-GHz circularly polarized dual-rhombic-loop traveling-wave rectifying antenna for low power-density wireless power transmission applications," *IEEE Trans. Microw. Theory Techn.*, vol. 51, no. 5, pp. 1548–1553, May 2003.

[5] C. Song, Y. Huang, P. Carter, J. Zhou, S. Yuan, Q. Xu, and M. Kod, "A novel six-band dual CP rectenna using improved impedance matching technique for ambient RF energy harvesting," *IEEE Trans. Antennas Propag.*, vol. 64, no. 7, pp. 3160–3171, Jul. 2016.

[6] S. Jiang and S. V. Georgakopoulos, "Optimum wireless powering of sensors embedded in concrete," *IEEE Trans. Antennas Propag.*, vol. 60, no. 2, pp. 1106–1113, Feb. 2012.

[7] K. M. Z. Shams and M. Ali, "Wireless power transmission to a buried sensor in concrete," *IEEE Sensors J.*, vol. 7, no. 12, pp. 1573–1577, Dec. 2007.

[8] K. Shafique, B. A. Khawaja, M. D. Khurram, S. M. Sibtain, Y. Siddiqui, M. Mustaqim, H. T. Chattha, and X. Yang, "Energy harvesting using a low-cost rectenna for Internet of Things (IoT) applications," *IEEE Access*, vol. 6, pp. 30932–30941, 2018.

[9] A. Okba, A. Takacs, and H. Aubert, "Compact flat dipole rectenna for IoT applications," *Prog. Electromagn. Res. C*, vol. 87, pp. 39–49, Sep. 2018.

[10] W. Lin, R. W. Ziolkowski, and J. Huang, "Electrically small, low-profile, highly efficient, huygens dipole rectennas for wirelessly powering Internet-of-Things devices," *IEEE Trans. Antennas Propag.*, vol. 67, no. 6, pp. 3670–3679, Jun. 2019.

[11] W. Zhao, K. Choi, S. Bauman, Z. Dilli, T. Salter, and M. Peckerar, "A radio-frequency energy harvesting scheme for use in low-power ad hoc distributed networks," *IEEE Trans. Circuits Syst. II, Exp. Briefs*, vol. 59, no. 9, pp. 573–577, Sep. 2012.

[12] M. N. Gadalla, M. Abdel-Rahman, and A. Shamim, "Design, optimization and fabrication of a 28.3 THz nano-rectenna for infrared detection and rectification," *Sci. Rep.*, vol. 4, no. 1, pp. 1–9, May 2015.

[13] T. Almoneef and O. M. Ramahi, "Dual-polarized multi-band infrared energy harvesting using h-shaped metasurface absorber," *Prog. Electromagn. Res. C*, vol. 76, pp. 1–10, Jul. 2017.

[14] T. S. Almoneef and O. M. Ramahi, "Metamaterial electromagnetic energy harvester with near unity efficiency," *Appl. Phys. Lett.*, vol. 106, no. 15, Apr. 2015, Art. no. 153902.

[15] T. S. Almoneef, F. Erkmen, M. A. Alotaibi, and O. M. Ramahi, "A new approach to microwave rectennas using tightly coupled antennas," *IEEE Trans. Antennas Propag.*, vol. 66, no. 4, pp. 1714–1724, Apr. 2018.

[16] J.-H. Ou, S. Y. Zheng, A. S. Andrenko, Y. Li, and H.-Z. Tan, "Novel time-domain Schottky diode modeling for microwave rectifier designs," *IEEE Trans. Circuits Syst. I, Reg. Papers*, vol. 65, no. 4, pp. 1234–1244, Apr. 2018.

[17] D. Masotti, A. Costanzo, P. Francia, M. Filippi, and A. Romani, "A load-modulated rectifier for RF micropower harvesting with start-up strategies," *IEEE Trans. Microw. Theory Techn.*, vol. 62, no. 4, pp. 994–1004, Apr. 2014.

[18] N. Zhu, R. W. Ziolkowski, and H. Xin, "A metamaterial-inspired, electrically small rectenna for high-efficiency, low power harvesting and scavenging at the global positioning system l1 frequency," *Appl. Phys. Lett.*, vol. 99, no. 11, Sep. 2011, Art. no. 114101.

[19] Y.-H. Suh and K. Chang, "A high-efficiency dual-frequency rectenna for 2.45-and 5.8-GHz wireless power transmission," *IEEE Trans. Microw. Theory Techn.*, vol. 50, no. 7, pp. 1784–1789, Jul. 2002.

[20] C. Song, Y. Huang, J. Zhou, J. Zhang, S. Yuan, and P. Carter, "A high-efficiency broadband rectenna for ambient wireless energy harvesting," *IEEE Trans. Antennas Propag.*, vol. 63, no. 8, pp. 3486–3495, Aug. 2015.

[21] C. Song, Y. Huang, J. Zhou, and P. Carter, "Improved ultrawideband rectennas using hybrid resistance compression technique," *IEEE Trans. Antennas Propag.*, vol. 65, no. 4, pp. 2057–2062, Apr. 2017.

[22] J. Kimionis, A. Collado, M. M. Tentzeris, and A. Georgiadis, "Octave and decade printed UWB rectifiers based on nonuniform transmission lines for energy harvesting," *IEEE Trans. Microw. Theory Techn.*, vol. 65, no. 11, pp. 4326–4334, Nov. 2017.

[23] A. Eid, J. G. D. Hester, J. Costantine, Y. Tawk, A. H. Ramadan, and M. M. Tentzeris, "A compact source–load agnostic flexible rectenna topology for IoT devices," *IEEE Trans. Antennas Propag.*, vol. 68, no. 4, pp. 2621–2629, Apr. 2020.

[24] S. Chandravanshi, S. S. Sarma, and M. J. Akhtar, "Design of triple band differential rectenna for RF energy harvesting," *IEEE Trans. Antennas Propag.*, vol. 66, no. 6, pp. 2716–2726, Jun. 2018.

[25] L. W. Epp, A. R. Khan, H. K. Smith, and R. P. Smith, "A compact dual-polarized 8.51-GHz rectenna for high-voltage (50 V) actuator applications," *IEEE Trans. Microw. Theory Techn.*, vol. 48, no. 1, pp. 111–120, Jan. 2000.

[26] T. S. Almoneef, F. Erkmen, and O. M. Ramahi, "Harvesting the energy of multi-polarized electromagnetic waves," *Sci. Rep.*, vol. 7, no. 1, pp. 1–14, Dec. 2017.

[27] S. Shen, C.-Y. Chiu, and R. D. Murch, "Multiport pixel rectenna for ambient RF energy harvesting," *IEEE Trans. Antennas Propag.*, vol. 66, no. 2, pp. 644–656, Feb. 2018.

[28] Y.-J. Ren and K. Chang, "Bow-tie retrodirective rectenna," *Electron. Lett.*, vol. 42, no. 4, pp. 191–192, Feb. 2006.

[29] S. Ahmed, Z. Zakaria, M. N. Husain, I. M. Ibrahim, and A. Alhegazi, "Efficient feeding geometries for rectenna design at 2.45 GHz," *Electron. Lett.*, vol. 53, no. 24, pp. 1585–1587, Nov. 2017.

[30] J. A. Hagerty, F. B. Helmbrecht, W. H. McCalpin, R. Zane, and Z. B. Popovic, "Recycling ambient microwave energy with broad-band rectenna arrays," *IEEE Trans. Microw. Theory Techn.*, vol. 52, no. 3, pp. 1014–1024, Mar. 2004.

[31] T. S. Almoneef, H. Sun, and O. M. Ramahi, "A 3-D folded dipole antenna array for far-field electromagnetic energy transfer," *IEEE Antennas Wireless Propag. Lett.*, vol. 15, pp. 1406–1409, 2016.

[32] C. Song, Y. Huang, J. Zhou, P. Carter, S. Yuan, Q. Xu, and Z. Fei, "Matching network elimination in broadband rectennas for high-efficiency wireless power transfer and energy harvesting," *IEEE Trans. Ind. Electron.*, vol. 64, no. 5, pp. 3950–3961, May 2017.

[33] (2019). *CST Microwave Studio Lab*. [Online]. Available: http://www.cst.com

[34] H. Sun, Y.-x. Guo, M. He, and Z. Zhong, "Design of a high-efficiency 2.45-GHz rectenna for low-input-power energy harvesting," *IEEE Antennas Wireless Propag. Lett.*, vol. 11, pp. 929–932, 2012.

[35] D. Sievenpiper, "High-impedance electromagnetic surfaces," Ph.D. dissertation, Dept. Elect. Eng., Univ. California Los Angeles, Los Angeles, CA, USA, 1999, pp. 2–3.

THAMER S. ALMONEEF (Member, IEEE) received the B.S. degree in electrical and computer engineering from Dalhousie University, Halifax, NS, Canada, in 2009, and the M.A.Sc. and Ph.D. degrees in electrical and computer engineering from the University of Waterloo, Waterloo, ON, Canada, in 2012 and 2017, respectively. In 2012, he was appointed as a Lecturer and was granted a scholarship from Prince Sattam Bin Abdulaziz University, Alkarj, Saudi Arabia, to pursue his Ph.D. studies, where he is currently an Assistant Professor with the Department of Electrical and Computer Engineering. He has authored and coauthored more than 35 refereed journals and conference papers. His research interests include antenna theory, metamaterials and its wide range applications, metamaterial absorbers, electrically small resonators, rectennas, microwave sensors and imagers, electromagnetic energy harvesting, and renewable energy.